Journal of Building Engineering 50 (2022) 104127

Contents lists available at ScienceDirect

Journal of Building Engineering

journal homepage: www.elsevier.com/locate/jobe

Effect of alkoxysilane on early age hydration in portland cement pastes

N. Husillos-Rodríguez [a,*], S. Martínez-Ramírez [b], R. Zarzuela [c], M.J. Mosquera [c], M. T. Blanco-Varela [a], I. Garcia-Lodeiro [a]

[a] Eduardo Torroja Institute IETcc-CSIC, Department of Materials, c/Serrano Galvache 4, 28033, Madrid, Spain
[b] Institute for the Structure of Matter IEM-CSIC, ENVIMED Department, C/Serrano 121, 28006, Madrid, Spain
[c] University of Cadiz, TEP-243 Nanomaterials Group. Department of Physical-Chemistry, 11510, Puerto Real, Spain

ARTICLE INFO

Keywords:
Consolidants
Alkoxysilanes
Silica oligomers
C–S–H
Hydration kinetics

ABSTRACT

Silanes added during mortar or concrete preparation, may modify the fresh state properties, hydration kinetics and mechanical strength of the final product. The effects of silanes on cement hydration have been widely studied in the literature, however, there is some controversy about its effect at short ages. The present study was undertaken to determine the effect of a TEOS-based alkoxysilane (UCA-T), produced by ultrasound-assisted pre-hydrolysis of an oligomeric precursor, on early age cement paste hydration. The nature of the processes modifying the various stages of cement hydration kinetics in the presence of the alkoxysilane was ascertained by analysing paste composition at several ages (defined on the grounds of calorimetric curve results) using XRD, TG-DTG, FTIR and Raman spectroscopy. The calorimetric curve of pastes containing UCA-T exhibited a new early age, pre-induction period exothermal peak, indicative of UCA-T hydrolysis, C_3A and C_3S dissolution and ettringite and C–S–H gel precipitation. Portlandite, however, did not precipitate but reacts with the $Si(OH)_4$ sourced from UCA-T hydrolysis to generate further C–S–H gel. The induction period following on that new exothermal peak was considerably longer than the period observed in the reference cement, an effect that intensified at higher UCA-T content.

1. Introduction

Silanes are being used ever more frequently to improve or modify some of the properties of portland cement mortars and concretes. The silanes most commonly applied to that purpose include tetraethoxysilane (TEOS) [1–3], its derivatives [4,5] or mixes of other silanes with TEOS [6].

TEOS or TEOS derivatives are produced with sol-gel processes. When applied as a sol to concrete or mortar surfaces they penetrate across the pore networks or into microcracks to consolidate the material [7,8]. TEOS penetration from the surface inward depends on the characteristics of the sol and the solid substrate [9,10]. The presence of liquid water or water vapour induces TEOS hydrolysis, giving rise to $Si(OH)_4$ (Equation (1)). Subsequent condensation of that compound (Equation (2)) generates colloidal silica that fills pores [11].

$$Si(O–CH_2–CH_3)_4 + 4H_2O \rightarrow Si(OH)_4 + 4CH_3–CH_2OH \quad (1)$$

* Corresponding author.
E-mail address: nuria.husillos@ietcc.csic.es (N. Husillos-Rodríguez).

https://doi.org/10.1016/j.jobe.2022.104127
Received 16 December 2021; Received in revised form 24 January 2022; Accepted 26 January 2022
Available online 8 February 2022

$$Si(OH)_4 \rightarrow SiO_2 + 2H_2O \quad (2)$$

In cementitious media the $Si(OH)_4$ groups resulting from TEOS hydrolysis may also react with portlandite [2,7,12] to generate new C–S–H, or with silanols in existing C–S–H, to lengthen the gel chain [7,13]. A similar effect is observed when silica fume or nanosilica is added to mortars and concretes to densify their structure, although there the end product is the outcome of a pozzolanic reaction. The latter technology is commonly applied to produce high strength concretes [14,15].

Be it said in that regard, that whilst the end product is C–S–H gel in both cases, the mechanisms and kinetics involved differ greatly. In pozzolanic reactions the stage that governs the process, SiO_2 dissolution, requires a highly basic medium to break the Si–O bond and release the silicate ions into the solution where they react with Ca^{2+}. C–S–H gel precipitates when the solution reaches saturation [16]. When alkoxysilanes are used, the $Si(OH)_4$ groups are released into the solution via hydrolysis (Equation (1)), very rapidly in basic media [17]. C–S–H precipitates when the silanol groups react with Ca^{2+} ions. Depending on the conditions prevailing in the medium, that reaction may compete with silica gel formation (Equation (2)) [13].

Recent studies on hydrated cement phases (such as ettringite, katoite, portlandite and C–S–H gel) stability in the presence of a base on TEOS oligomer product at saturated RH and ambient temperature have determined the phases that react with the oligomer to generate new stable phases [13].

According to the literature, when silanes are used in mortar or concrete preparation, depending on their composition and structure, they may modify the fresh state properties, hydration kinetics and mechanical strength of the end product [18–25].

Cai et al. [19], for instance, observed that TEOS lengthens the induction period in cement paste (w/c = 0.5; 1% TEOS) and delays the maximum heat flow at peak hydration. They attributed those effects to a lack of sufficient water, consumed in TEOS hydrolysis. Kong et al. [18], in contrast, observed a similar delay when adding alkyl silanes but not TEOS to the mix. Whilst the former remained in solution for several hours in a medium simulating the aqueous phase of concrete, TEOS concentration declined rapidly. The authors inferred that whereas hydrolysed alkyl silanes gradually adsorbed onto the surface of the cement grains, lengthening the cement paste induction period, TEOS hydrolysed quickly. The resulting silanol groups reacted rapidly with the Si–OH groups on the grain surface, prompting TEOS adsorption or precipitation on that surface, thereby obstructing water access and hence dissolution [18]. Nonetheless, in the presence of TEOS the sole change observed in the hydrated paste calorimetric curves was lower heat of hydration at 120 h, whilst the duration of the induction period remained unmodified.

The chemical formula of the alkyl silanes added to fresh state mortars or concretes also affects cement hydration. Adding amino-, vinyl- and epoxy-silanes to the mortar mix, Feng et al. [20] reported a delay in hydration, deemed to possibly be due to silane adsorption onto the cement grain surface. Adding silanols in the form of oligomers or nanoparticles mitigated delays in hydration. The same authors found that procedure to raise flexural and in some cases compressive strength [20]. Kooestani [21], in turn, observed a mix of TEOS and methyl trimethoxy silane (MTMS) did not enhance mechanical strength when added to cement mortars, but did it when either was included separately.

Chen et al. [22] studied the effect of three (1%) silanes (aminopropyltriethoxysilane, glycidylpropyltrimethoxysilane and methacryloyloxypropyltrimethoxysilane) on cement hydration (w/c = 0.3), measuring resistivity, isothermal conduction calorimetry and mechanical strength. They found the silanes studied to lower initial dissolution due to the water consumption inherent in silane hydrolysis. Analysing the effect of pre-hydrolysis of the alkyl silanes on the rate of heat released in cement hydration, they found induction period lengthening to be accentuated at higher degrees of pre-hydrolysis, countering the results reported by Feng et al. [20]. They deemed that silanol adherence to the surfaces of incipient $Ca(OH)_2$ (CH) or C–S–H via hydrogen bridges obstructed contact with the water. When hydration was renewed resistivity rose, but less in the pastes bearing siloxanes. That they attributed to the structural densification induced by the hydrolysed silanes, which behaved like a glue, and to the formation of C–S–H gel in the reaction between portlandite and silanol groups. Portlandite concentration and paste porosity were observed to decline and mechanical strength to rise in the 28 d pre-hydrolised silanes-bearing cements relative to the non-silanes reference.

Casagrande et al. [26] studied cement pastes with a partial substitution of superplasticizer by silanes (tetraethoxysilane, 3-Glycidoxypropylmethoxysale and aminoethylaminopropyltrimethoxysilane) using isothermal calorimetry. The result in the case of TEOS was an acceleration on the kinetics of hydration and an increase in the heat of hydration at 120 h compared to the reference. This was attributed to the silanes interaction with the Ca^{+2} and OH^- ions of the solution, which gives rise to the precipitation/formation of C–S–H. García-Lodeiro et al. [27] incorporated a combination of a TEOS and PDMS oligomer into a mortar to obtain a hydrophobic mortar. The calorimetric studies revealed an acceleration of the early hydration kinetics of cement, a lower initial heat of dissolution, an increase in heat released during the induction period, and a reduction in the total heat released after seven days of hydration. Collodetti et al. [28] studied the hydration of cement pastes by adding amino and epoxy silanes and their results showed how silanes interfere on the early ages of hydration of cement pastes. Švegl et al. [29] reported that certain aminosilanes can improve the spreading (diffusion) of cement paste and reduce water demand.

Thus, there is reasonable agreement in the literature on the effect of silanes when applied to the surface of hardened mortars and concretes, but there is some controversy and contradictory results on the effects of silanes when they are incorporated in mass on the hydration of Portland cement, as well as on the final properties of mortars or concretes.

The present study was undertaken to determine the effect of a TEOS-based prehydrolysed alkoxysilane (UCA-T), produced by ultrasound-assisted pre-hydrolysis of an oligomeric precursor, on early age cement paste hydration. The nature of the processes modifying the various stages of cement hydration kinetics in the presence of the alkoxysilane was ascertained by analysing paste composition at several ages (defined on the grounds of calorimetric curve results) using XRD, TG-DTG, FTIR and Raman spectroscopy.

2. Experimental

2.1. Materials

The effect of UCA-T on early cement hydration was studied with the white cement (CEM BL I 52.5) described in Table 1 (XRF-determined chemical composition). According to mineralogical characterization the cement contains alite, belite, tricalcium aluminate and anhydrite as main crystalline phases (XRD and FTIR of cement are reported as S2 in supplementary material).

The alkoxysilane used (UCA-T) contained a mix of (1) an oligomeric ethoxysilane (TES40, Wacker) with an average chain length of five Si–O units; (2) n-octylamine (98%, Sigma-Aldrich), added as a hydrolysis catalyst and surfactant used to raise alkoxysilane miscibility with water; and (3) a small amount of de-ionized water (0.5% v/v).

An ultrasound probe was used to blend the components into a uniform mix and pre-hydrolyse the oligomer. A detailed description of the process involved in synthesis is given in Refs. [23,24].

2.2. Methodology

Three cement pastes were prepared, with a w/c = 0.35 (standard consistency). The reference (PS) was mixed with water, whereas the other two pastes also contained 3% and 6% of UCA-T (by weight of cement) labeled respectively as PS-3% and PS-6%. The pastes were analysed as described below.

a) Hydration kinetics were monitored during the first 7 d with isothermal conduction calorimetry, plotting the heat flow (HF) and total heat released (TH) curves with the data delivered by a TAM Air calorimeter. Test samples were prepared by mixing 20 g of cement and deionised water as the hydration medium (liquid/solid ratio = 0.35). The mixing sequence was 90 s at 168 rpm followed by a 60 s rest and remixing for a further 90 s at 168 rpm. The UCA-T was added in the last 90 s. Hydration was monitored in 5 g aliquots of each mix, placed in the calorimeter immediately after preparation. Upon conclusion of the calorimetric test the samples were removed, ground to a particle size of <45 μm and soaked in isopropanol as described in Ref. [25] to detain hydration. These samples were then characterised with XRD, FTIR and TG/DTG.
b) Very early stage hydration was monitored in the three pastes with Raman spectroscopy. White cement samples weighing 0.001 g were set inside a sample holder and without varying the distance from the microscope mixed (with the tip of the pipette to ensure homogeneity) with 0.35 μL of distilled water or water bearing UCA-T for 30 s, after which the holder was lidded. Micro-Raman spectra were then recorded at the same point at t = 3 min and t = 4 h.
c) Cement hydration in the presence of UCA-T was analysed on pastes with the same composition prepared to the same procedure as for isothermal conduction calorimetry. Samples were immersed in water in sealed bags at 25 °C, removed at times determined in keeping with the calorimetric curve results (Table 2), ground and treated with isopropanol to detain hydration as described above. The resulting samples were analysed with XRD, FTIR and TG/DTG.

XRD analyses were performed on a Bruker D8 Advance diffractometer consisting in a 2.2 kW generator and a copper anode X-ray tube (CuKα1 radiation: 1.5406 Å and CuKα2: 1.5444 Å) operating at 40 kV and 30 mA and fitted with a 0.5° fixed divergence slit and a non-monochromatic Lynxeye super speed detector bearing a 3 mm anti-scatter slit, a 2.5° secondary Soller slit and a 0.5% Ni K-beta filter. Readings were taken for approximately 1 h per diffractogram over a 2θ angular range of 5°–60° with a 0.02° step size.

Samples pressed into KBr pellets were scanned (10 scans per sample) to record their infrared spectra with a Nicolet 6700 spectrometer in the 4000 cm^{-1} to 400 cm^{-1} range at a spectral resolution of 4 cm^{-1}.

Thermogravimetric heat flow was determined on a TA SDT Q600 analyser with platinum crucibles (empties were used as a reference). The samples were heated to 1050 °C at a 10 °C/min rate in a nitrogen atmosphere.

The Raman spectra were recorded in a RM 2000 Renishaw Raman microscopy with red (λ = 633 nm) laser excitation under the following conditions: a) three 10 s cumulative scans at 4000 cm^{-1} to 100 cm^{-1}, 25 mW laser power and 50x magnification (recording time for this spectrum, 2 min 30 s); and b) three 10 s cumulative scans recorded at 1200 cm^{-1} to 100 cm^{-1}, 25 mW laser power and 50x magnification (recording time for this spectrum, 1 min 30 s).

3. Results

3.1. Study of the PC pastes hydration using isothermal conduction calorimetry

The calorimetric curves for the white cement paste reference (PS) and those with 3% (PS-3%) or 6% (PS-6%) of UCA-T are reproduced in Fig. 1. In the first few minutes of hydration cement moistening induced the initial dissolution of sulfates, aluminates and alite. The initially high heat flow rate recorded in the reference declined gradually (Fig. 1(a)) to a minimum at 54 min, when the induction period began. Adding UCA-T lowered the initial heat flow rate, which declined after 12 min in PS-3% and 8 min in PS-6% and then rose until t = 29 min in both. That was followed by a steady decline up to t = 2 h and t = 4 h 21 min. The respective induction periods preceding the hydration peak characteristic of cement pastes, which was particularly broad in the 6% UCA-T sample, began at

Table 1
XRF-determined chemical composition of CEM BL I 52.5 (wt% oxides).

	CaO	Al_2O_3	SiO_2	SO_3	MgO	Fe_2O_3	Na_2O	K_2O	TiO_2	LOI[a]
CEM BL I 52.5R	64.07	3.79	21.65	2.16	0.36	0.24	0.08	0.21	0.08	4.18

[a] LOI: Loss on ignition at 1000 °C.

Table 2
Hydration detention times based on calorimetric curve results (Fig. 1(a)).

Sample	UCA-T content	Hydration detention time						
PS	0%	[a]54 min	[b]4 h 48 min	8 h 6 min	24 h	48 h		
PS-3%	3%	12 min	29 min	[a]2 h	[b]6 h	24 h		
PS-6%	6%	8 min	29 min	47 min	[a]4 h 21 min	6 h 4 min	[b]16 h 13 min	24 h

[a] Start of induction period.
[b] Maximum acceleration-deceleration peak.

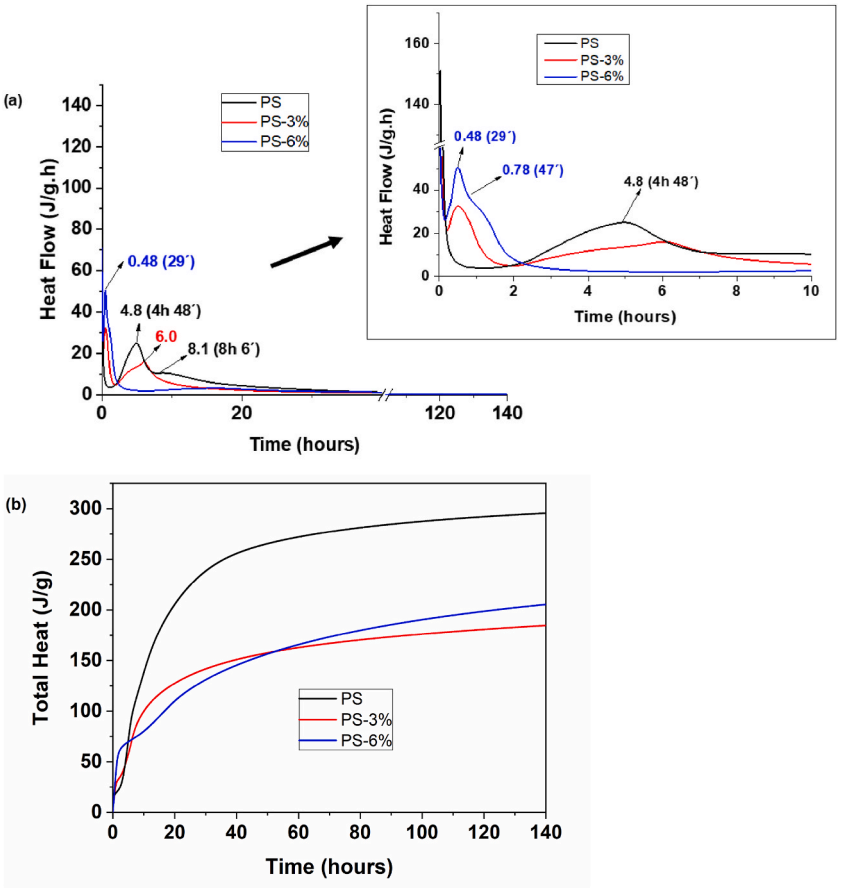

Fig. 1. (a) Heat flow and (b) total heat of hydration in PC pastes with 0% (PS), 3% (PS-3%) or 6% (PS-6%) of UCA-T.

the aforementioned times.

The alterations in heat flow gave rise to exothermal pre-induction peaks on the calorimetric curves for the pastes containing UCA-T that were absent in the reference.

The delays in the onset of induction retarded the acceleration-deceleration stage in which alite dissolution and C–S–H precipitation peak. Other authors [15,19] reported a longer induction period in pastes with 1% TEOS, which they attributed to the presence of less water in the medium due to its consumption in TEOS hydrolysis. None observed the aforementioned additional peaks, however, which in this study appeared in the first 2 h–4 h.

The slope of the acceleration curve for the main cement hydration peak (Fig. 1(a)) in the UCA-T pastes was smaller than observed for the reference (cement + water). Similarly, the sulfate depletion peak, very intense in PS (at 8 h 6 min), was practically absent in the other two pastes.

Upon conclusion of the calorimetric trial after 7 d, the heat of hydration released by the 3% UCA-T pastes came to 188 J/g and by the 6% pastes to 212 J/g, respectively 37% and 29% less than the 299 J/g released by the reference (Fig. 1(b)), denoting a lower degree of hydration in these materials, which is in agreement with the results found by Kong et al. [18], and in disagreement with those found by Casagrande et al. [26], this discordance could be explained by the fact that the reference cement paste in Ref. [26] includes polycarboxylate, which is known that induces a delay in the initial hydration of cement paste [30,31] and TEOS is partially replacing this admixture, so that the effect of TEOS would be confused with the effect caused by a reduction in the proportion of polycarboxylate.

The 7 d diffractograms for the reference (PS) and experimental (PS-3% and PS-6%) pastes reproduced in Fig. 2 show the reflections for the crystalline products of white cement hydration: ettringite (e) and portlandite (p), along with traces of the anhydrous cement phases alite (A) and belite (B). The intensity of the portlandite peaks declined steeply and the alite and belite peaks grew with rising UCA-T content relative to the reference, a finding consistent with the lower 7 d heat of hydration released by the latter. All the samples generated peaks for calcite (c) and monocarboaluminate (mc).

According to the TG findings (Table 3, Fig. 3), mass loss at temperatures of up to 200 °C was similar in the two 7 d hydrated UCA-T pastes and smaller than in the reference. At those temperatures the C–S–H gel released some water [13,32], whilst ettringite [33] and AFm [34] dehydrated. Part of the water or OH in C–S–H gel was lost at 200 °C to 390 °C [13,32] and AFm phases dehydroxylated (at 200 °C to 390 °C in calcium monocarboaluminate hydrate) [34,35]. Mass loss in that temperature range was also observed to be greater in PS than in PS-3% or PS-6%.

The greatest differences were found in portlandite dehydroxylation-related loss, which was two-fold larger in PS than in PS-6% (Table 3). The higher the UCA-T content in the pastes, the lower was portlandite content (data consistent with the XRD). In addition, the portlandite dehydroxylation peak on the DTG curve was narrower and more symmetric and reached a lower maximum temperature in the UCA-T-bearing samples than in the reference.

Two mass losses were observed in the ranges 600 °C–650 °C and 690 °C–720 °C, interpreted to be due to the release of CO_2 by monocarboaluminate and calcite [32], (present in the anhydrous cement or sourced from portlandite carbonation). As decarbonation-induced losses were similar in the three samples, the decline in the portlandite content in the UCA-T samples was not attributable to its carbonation.

Nonetheless, the decline in some of the portlandite might be explained by its reaction with UCA-T [12,13]. Inasmuch as UCA-T has an SiO_2 content of around 40% [12], the 3% UCA-T pastes had around 0.98% and the 6% UCA-T pastes 1.98% additional SiO_2 (mixing water factored into the calculations) (Calcules are shown in supplementary material as S3). If after UCA-T hydrolysis the silanol groups were assumed to react in their entirety with the calcium ions in the aqueous phase to form C–S–H, the portlandite content in paste PS-3% would decline by 1.2% and in PS-6% by 2.4% (assuming a Ca/Si molar ratio of 1–2 in the C–S–H forming). That lower portlandite content in the pastes due to the reaction with UCA-T would explain only part of the difference with the content in the reference. From this, it can inferred the influence of the decrease in alite and belite hydration.

Mass loss from 750-770 °C–1000 °C was attributed to wollastonite formation, a result of the reaction between partially hydroxylated silica and lime [32].

Both total mass loss and loss of bound water (25 °C–500 °C) declined at higher UCA-T content, confirming the calorimetric and XRD findings and denoting a lower degree of reaction at the test age in the pastes with higher UCA-T contents.

3.2. Raman spectroscopy

The Raman spectra of the PS and PS-3% samples are shown in the Supplementary Material (S4.1 y S4.2). The PS sample shows the characteristic signals of the calcium silicate phases of an anhydrous cement, alite and belite (800-900 cm^{-1}) and calcite (1085 cm^{-1}) [36].

A comparison of the Raman spectra for the first 15 min of hydration in samples PS and PS-3% (Fig. 4(a)) showed that the water-hydrated cement contained AFm phases (1100 cm^{-1} to 900 cm^{-1}) [37,38], the signals for which were wider and less intense in paste moistened with water + UCA-T. After 2 h (Fig. 4(b)), ettringite formation was clearly observed in PS, whereas the aforementioned wide signal persisted in PS-3%.

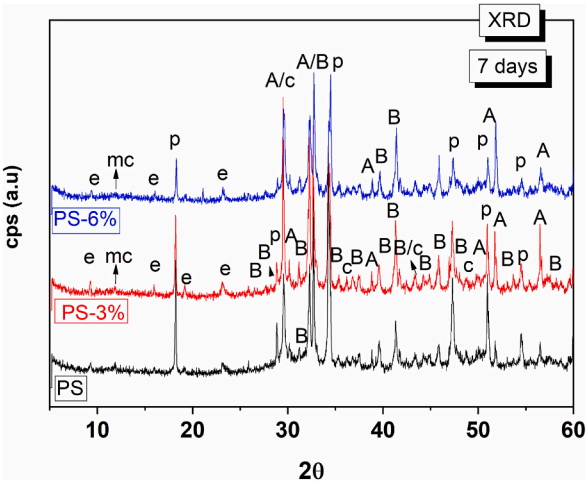

Fig. 2. XRD patterns for 7 d hydrated PS, PS-3% and PS-6% (legend: A: alite (C_3S) (COD 1540704); B: belite (C_2S) (COD 9012789); c: calcite ($CaCO_3$) (COD 9016022); mc: monocarboaluminate $C_4A\check{C}H_{11}$ (COD 2007668); p: portlandite ($Ca(OH)_2$ (COD 1008781); e: ettringite (COD7020139).

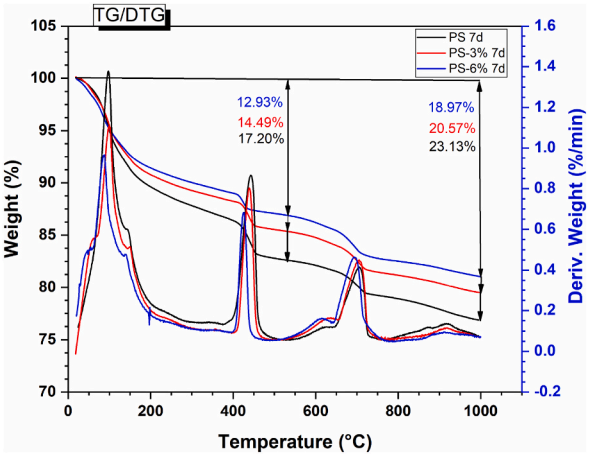

Fig. 3. TG and DTG curves for 7-day hydrated PS (reference), PS-3% (3% UCA-T) and PS-6% (6% UCAT).

Table 3
Mass loss (%) calculated from TG data at different temperature ranges and percentages of $Ca(OH)_2$ and $CaCO_3$.

	Temperature range (°C)					wt% of phases and bound water (25–500 °C)			
System	25–200	200–390	390–500	500–775	775–1000	Total loss	$Ca(OH)_2$	$CaCO_3$	Bound water
PS	10.39	3.09	3.72	3.72	2.21	23.13	15.29	8.45	17.20
PS-3%	9.26	2.34	2.88	4.24	1.85	20.57	11.84	9.64	14.48
PS-6%	8.59	2.34	1.99	4.44	1.6	18.97	8.18	10.09	12.92

3.3. Effect of UCA-T on early age hydration

3.3.1. Reference cement (PS: cement + water)

In order to have a reference system, the samples consisting in the mixture of cement + water (without the alcoxysilane UCA-T), were characterised by XRD, FTIR and TG/DTG, at different short ages (from 54 min to 48 h) based on the ages defined on the isothermal calorimetric curves (Table 2, Fig. 1(a)). The results obtained are included in the Suplementary Materials (See Fig. (S5.1-S5.4) and Table S1).

3.3.2. Cement with 3% UCA-T (PS-3%)

The diffractograms for the 12 min and 29 min samples (Fig. 5) showed scarcely any difference with the anhydrous cement (See Fig S5.1, in SM): intense signals were detected for the anhydrous calcium silicates as well as for C_3A, anhydrite and calcite. No reflections for any hydrated phase, even gypsum, were observed. The 2 h XRD patterns (beginning of the induction period) varied scantly from the earlier curves, with low intensity signals for ettringite but not for portlandite. The diffractogram after 6 h of hydration (time of maximum heat flow on the calorimetric curve) contained intense reflections for alite, belite and C_3A, whilst the ettringite signal grew and a line identified with portlandite was detected. The 24 h XRD pattern had very low intensity (traces) signals for C_3A, the lines for portlandite and ettringite grew and while the alite reflections declined intense diffraction lines for silicates persisted (Fig. 5).

The FTIR spectra for PS-3% at the hydration times specified in Table 2 are reproduced in S6 in supplementary material.

The 12 min and 29 min spectra were very similar to one another but differed from the spectrum for anhydrous cement (See Fig S5.2, in SM) in the S–O asymmetric stretching vibration region (1050-1200 cm^{-1}). That band was attributable to the anhydrite in the anhydrous cement and gypsum in the two PS-3% pastes at the aforementioned hydration times. Both PS-3% spectra also exhibited a very weak band at around 3640 cm^{-1} attributable to the O–H asymmetric stretching vibration generated by portlandite, a hydrate not identified on the XRD patterns due perhaps to its minor presence or poor crystallinity. The spectra for the 2 h and 6 h pastes (beginning of induction period and peak hydration-induced heat flow) showed no perceptible change in the intensity in the small portlandite band at around 3640 cm^{-1} (S6 in Suplementary material), which may have recrystallised in the 6 h sample, when it was identified on the XRD pattern. The intensity of that band rose visibly in the 24 h spectrum.

The main ettringite band in the S–O asymmetric stretching vibration region (1050-1200 cm^{-1}) was clearly identifiable (not overlapping with gypsum) in the 2 h paste and observed in the same position in the 6 h and 24 h samples (Figura 6). Those observations were consistent with the XRD and Raman findings (Figs. 5 and 4).

The main silicate band, generated by Si–O antisymmetric vibrations, evolves slowly in the first 6 h of hydration (Fig. 6), the highest peak shifted from 923 cm^{-1} to a higher wavenumber, appearing a new band at 980 cm^{-1} characteristic of C–S–H gel [13,39]. Those findings attested to alite hydration while suggesting that the paucity of portlandite in the samples may have been due to its reaction with the $Si(OH)_4$ released from the UCA-T hydrolysis. The Si–O stretching vibration signals generated by SiOH groups in $Si(OH)_4$ are also located in this region, although at a lower wavenumber (960 cm^{-1} to 965 cm^{-1}) [40]. Nonetheless, the width and shift in the band

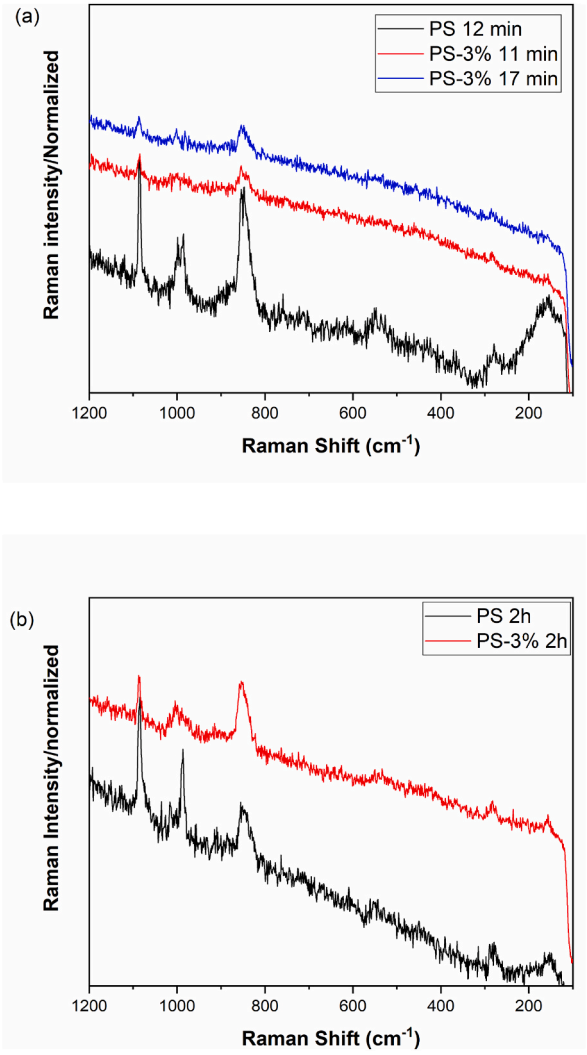

Fig. 4. Raman spectra for 15 min (a) and 2 h (b) samples hydrated with H_2O (PS) or H_2O + 3% UCA-T (PS-3%) (λ = 633 nm).

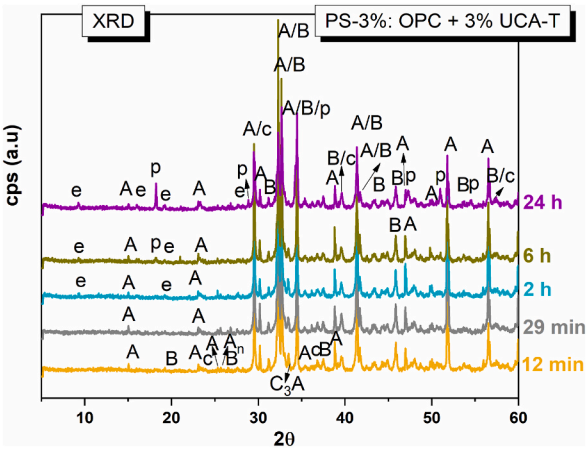

Fig. 5. Early age diffractograms for hydrated cement pastes containing 3% UCA-T. (legend: A: alite (C_3S) (COD 1540704); B: belite (C_2S) (COD 9012789); C_3A: tricalcium aluminate (COD 9015966); c: calcite ($CaCO_3$) (COD 9016022); A_n: anhydrite ($CaSO_4$) (COD 5000040); p: portlandite ($Ca(OH)_2$ (COD 1008781); e: ettringite (COD7020139).

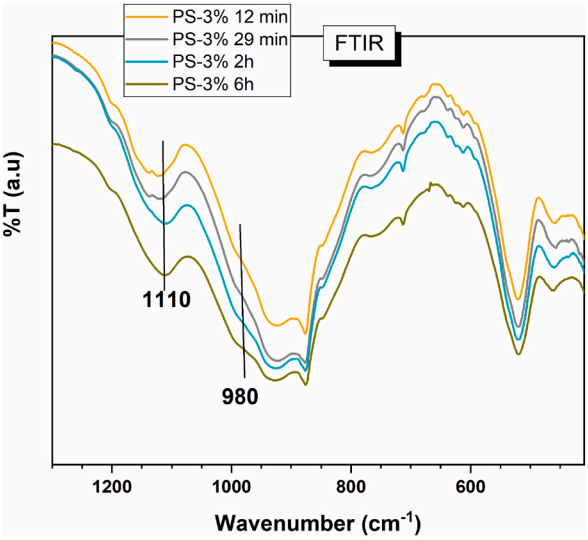

Fig. 6. FTIR spectra for 3% UCA-T paste: detail for the first 6 h.

observed rule out that interpretation.

A comparison of the FTIR spectra for the PS pastes at the peak heat flow time (PS 4 h 48 min and the PS-3% paste at the beginning of the induction period (2 h) (Fig. 7), showed that the band characteristic of portlandite was much more intense in the former, denoting greater alite hydration. And although the differences in the silicate bands were minor, the 982 cm^{-1} component characteristic of C–S–H gel was somewhat more intense in PS-3%. Those findings suggested that the 2 h PS-3% pasted contained more C–S–H gel than the 4 h 48 min PS paste and that UCA-T did not retard alite hydration in that interval but rather that the portlandite generated in the reaction was subsequently consumed because it reacted with the oligomers hydrolysed from the silane, generating C–S–H.

The TG/DTG thermograms for the hydrated PS-3% pastes (Fig. 8 and details in supplementary material as S7) exhibited an initial peak that shifted from 68 °C to 80 °C and grew in intensity with hydration time. The gypsum peak (120°C) grew slightly between 12 min and 29 min to later decline significantly and overlap with the signal for ettringite, which was observed to be more intense after 2 h of hydration. The peaks at around 400 °C in the curves for the 12 min and 29 min pastes, possibly attributable to traces of amorphous portlandite, disappeared in the 2 h sample. The thermogram for paste PS-3% 2 h exhibited two wide peaks (located between 400 °C-600 °C) of uncertain identification that preceded the calcite decarbonation peak. As Fig. 8 and Table 4 show, hydration barely progressed between 12 min and 29 min but much more rapidly between 29 min and 2 h. In contrast, the decarbonation signals remained very similar throughout. The losses at the various temperature ranges in paste PS-3% at the beginning of the induction period (2 h, Table 4) were slightly higher than observed for PS at maximum heat flow (4 h 48 min, Table S1 in SM). Those data confirmed the FTIR results and that alite hydration was not inhibited by UCA-T in this initial period.

The 6 h (peak hydration-induced heat flow) TG/DTG curves were similar to the ones recorded at the beginning of the induction period (2 h), although a small loss was observed in the portlandite region and another after the main decarbonation peak, possibly induced by water from the hydroxylated silica gel in its reaction with the Ca^{2+} ions to generate wollastonite. The same signals were more intense on the 24 h TG curve and the ones attributable to an AFm phase, possibly carboaluminate which might be present in the sample in small quantities or as an amorphous compound, for it was not detected with XRD.

3.3.3. Cement with 6% UCA-T (PS-6%)

The 8 min and 29 min (start and maximum heat flow times of the additional hydration peak observed in the samples containing UCA-T) diffractograms (Fig. 9) exhibited reflections for the anhydrous cement phases alite, belite, C_3A, gypsum and anhydrite. Anhydrous phase reflection intensity did not decline significantly in the 47 min mix (which is the time corresponding to the shoulder on the new exothermal peak on the PS-6% isothermal calorimetric curve). Whilst the PS-6% 47 min. XRD pattern, exhibited incipient signals for ettringite, no lines attributable to portlandite were observed. The diffractograms for the 4 h 21 min and 6 h 4 min (both in the induction period) PS-6% pastes were very similar: portlandite peaks were first detected after 6 h and the ettringite peaks rose in intensity. The reflections for the anhydrous phases remained intense, however.

The signals for ettringite and portlandite grew more intense on the 16 h 13 min and 24 h PS-6% pastes, while the reflection attributed to C_3A disappeared and those due to alite shrank in the latter. Nonetheless, substantial amounts of anhydrous silicates were still detected.

FTIR, confirm the XRD results, related to the first detection and the evolution with time of both portlandite (see S8 in SM).

On the spectra for the samples hydrated up to the beginning of the induction period (4 h 21 min) (Fig. 10) the main band for anhydrous silicates (923 cm^{-1}) shifted to steadily higher wavenumbers. The band characteristic of C–S–H gel (970 cm^{-1} to 990 cm^{-1}), in turn, grew with hydration time and became even more intense at later times.

Irrespective of hydration time, all the TG/DTG curves for the PS-6% pastes contained a peak indicative of water loss with a

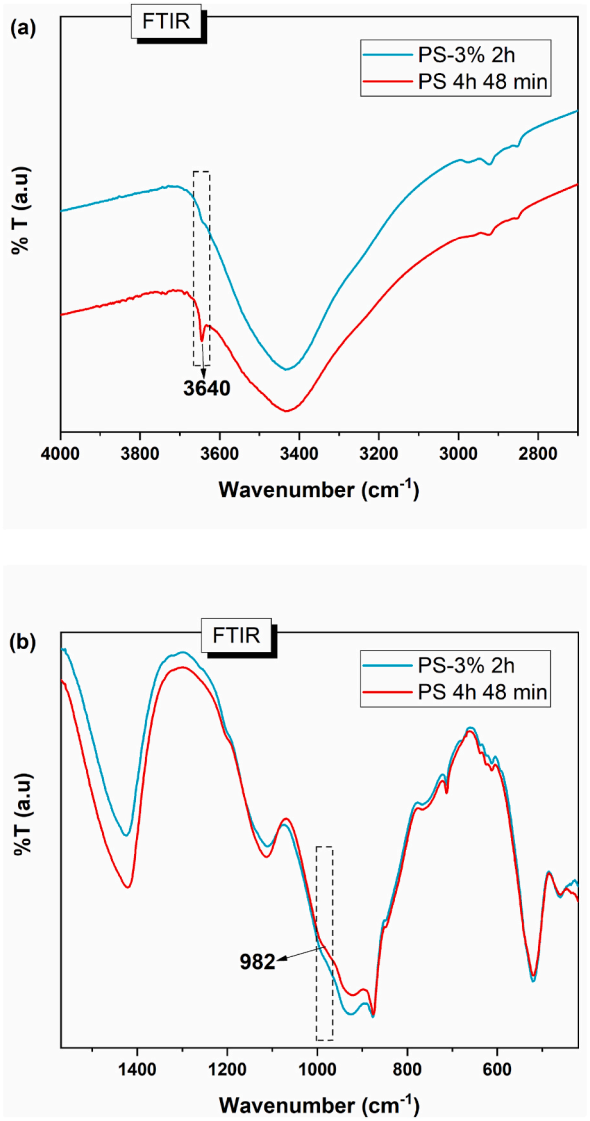

Fig. 7. FTIR spectra for 4 h 48 min PS and 2 h PS-3% pastes: (a) 4000 cm^{-1} to 2600 cm^{-1}; (b) 1600 cm^{-1} to 500 cm^{-1}.

maximum that shifted over time from 69.7 °C to 84.4 °C. That behaviour was attributable to ettringite dehydroxylation, inasmuch as more and larger crystals would form at longer hydration times (Table 5, Fig. 11, more details in supplementary material S9).

The thermograms recorded at the beginning of the additional exothermal hydration peak (8 min), at the maximum heat flow (29 min) and with the appearance of the shoulder (47 min) exhibited mass loss at 120 °C attributable to gypsum. The respective signal declined with time and disappeared from the curve recorded at the beginning of the induction period (4 h 21 min sample).

The TG/DTG thermograms for the two samples recorded during the induction period (4 h 21 min and 6 h 4 min), as well as for the two latest samples, exhibited signals in the 150 °C area attributable to water loss in AFm phases, very likely monocarboaluminate, as mass losses (500–600 °C region) are also observed.

The signal characteristic of portlandite dehydroxylation appeared with minor intensity on the 8 min DTG curve for PS-6%. While not visible on the 29 min, 47 min or 4 h 21 min curves, it reappeared on the 6 h 4 min thermogram and increased in intensity thereafter (see details in supplementary material as S9).

The signals due to the loss of CO_2 from decarbonation of $CaCO_3$ or monocarboaluminate grew with rising hydration time.

4. Discussion

As the calorimetric curves in Fig. 1 show, adding UCA-T to cement paste altered hydration substantially from the outset. The samples bearing UCA-T exhibited an additional exothermal peak not described in the literature before the outset of induction period. The nature of that peak was studied. The exothermal process denoting the initial C_3A and C_3S hydration [41], appeared to be hindered

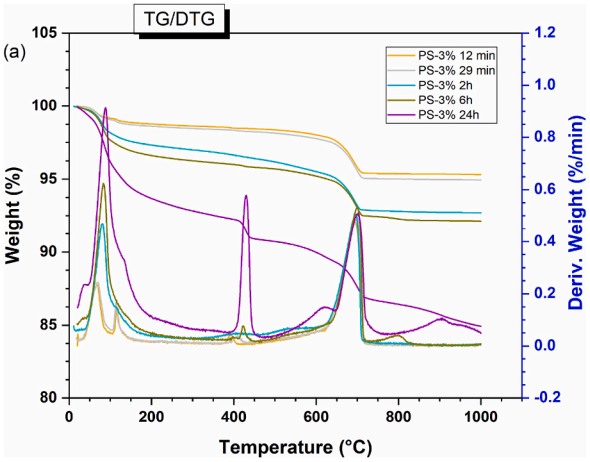

Fig. 8. TG/DTG curves for PS-3% pastes by different hydration time (a).

Table 4
Mass loss (%) in paste PS-3% calculated from TG by temperature range and hydration time and $Ca(OH)_2$ and $CaCO_3$ content (%) by hydration time.

T (°C)/PS-3%	25–200	200–390	390–500	500–750	750–1000	Total weight loss	$Ca(OH)_2$	$CaCO_3$	Bound water
12 min	1.23	0.21	0.19	2.98	0.04	4.68	0.78	6.77	1.63
29 min	1.38	0.26	0.22	3.11	0.08	5.04	0.90	7.07	1.86
2 h	2.67	0.64	0.5	3.33	0.15	7.31	2.05	7.57	3.81
6 h	3.38	0.59	0.32	3.24	0.33	7.88	1.31	7.36	4.29
24 h	6.25	1.4	1.55	4.06	1.54	15.07	6.37	9.23	9.2

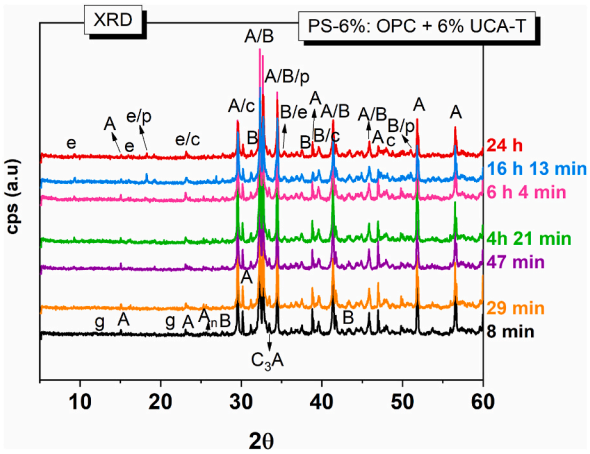

Fig. 9. Early age diffractograms for hydrated cement pastes containing 6% UCA-T. (legend: A: alite (C_3S) (COD 1540704); B: belite (C_2S) (COD 9012789); C_3A: tricalcium aluminate (COD 9015966); c: calcite ($CaCO_3$) (COD 9016022); g: gypsum ($CaSO_4$. $2H_2O$) (COD 9015350) A_n: anhydrite ($CaSO_4$) (COD 5000040); p: portlandite ($Ca(OH)_2$ (COD 1008781); e: ettringite (COD7020139).

by the presence of UCA-T. The silane's non-polar oligomers might obstruct water access to the cement particles, more intensely at higher UCA-T content (more in PS-6% than in PS-3%). Evidence of such obstruction lies in the amount of heat released by the three pastes in the first 8 min: PS-6% just half and PS-3% just 75% of the amount released by reference PS. Nonetheless, heat flow rose in sample PS-6% after 8 min and in PS-3% after 12 min, peaking at 29 min, whilst the flow in PS declined steadily. At 54 min, when its induction period began, PS had not yet reached the heat released by PS-6% after 29 min (Table S2 in supplementary material).

The calorimetric findings further showed that adding UCA-T to the pastes retarded the beginning of the induction period from 54 min in PS to 2 h in PS-3% and 4 h 21 min in PS-6%. According to the literature, adding TEOS lengthens the induction period in cement paste, retarding peak hydration heat flow. That delay has been attributed to the decline in water content due to its consumption in TEOS hydrolysis [19]. Other authors [24] reported no change whatsoever in the earliest stages, but lower heat of hydration after 120 h, which they interpreted to be due to a decline in cement dissolution rate in the wake of the adsorption of the silanol groups in TEOS onto

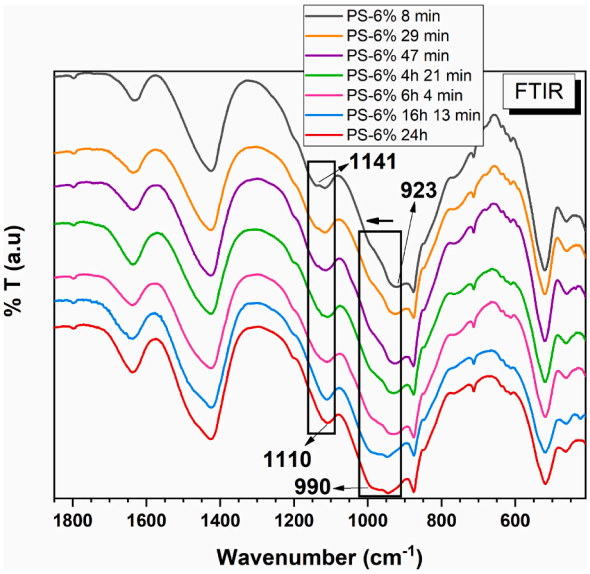

Fig. 10. Early age FTIR spectra for hydrated cement PS-6% pastes (1800 cm^{-1} to 400 cm^{-1}).

Table 5
Mass loss (%) in paste PS-6% calculated from TG by temperature range and hydration time.

T (°C)/PS-6%	25–200	200–390	390–500	500–750	750–1000	Total mass loss	$Ca(OH)_2$	$CaCO_3$	Bound water
8 min	1.23	0.27	0.18	2.66	0.03	4.36	0.74	6.14	1.68
29 min	2.23	0.40	0.22	3.06	0.09	6.00	0.90	7.16	2.85
47 min	2.73	0.49	0.25	3.05	0.07	6.62	1.03	7.11	3.47
4 h 21 min	4.05	0.77	0.41	3.44	0.77	9.48	1.70	7.82	5.23
6 h 4 min	4.32	0.82	0.47	3.49	0.51	9.62	1.93	7.93	5.61
16 h 13 min	7.29	1.59	1.01	4.16	1.32	15.4	4.15	9.45	8.47
24 h	6.17	1.33	0.97	4.51	1.21	14.2	3.99	9.79	12.92

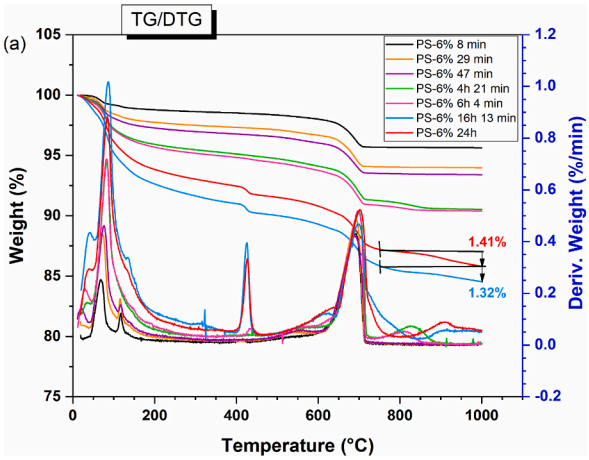

Fig. 11. TG/DTG curves for PS-6% pastes: (a) at all the ages studied.

the grain surfaces.

The samples bearing UCA-T, however, exhibited a longer pre-induction period (up to 4 h 21 min in PS-6%) with the appearance of the additional exothermal peak.

The aforementioned pre-induction peak, observed at 29 min in samples PS-3% and PS-6%, was more intense in the latter and

possibly due to TEOS hydrolysis, an extremely exothermal process (12.7 kJ/mol) [42]. In light of the proportion of UCA-T in the pastes, the contribution of UCA-T hydrolysis to the total heat of hydration would be 5.22 Jules per gramme of cement in the paste containing 3% UCA-T (by cement weight, PS-3%) and 10.44 J/g in the 6 wt% paste (PS-6%). That would explain the intensely exothermal pre-induction period peak on the calorimetric curve in the two samples only partially, therefore inferring the presence of other simultaneous exothermal reactions such as cement phases dissolution.

While etoxysilanes hydrolysis is a slow process in the absence of catalysts [7,12], it is hastened in basic media, and the rate constant of that reaction rises linearly with OH^- concentration, although it also depends on the H_2O/TEOS ratio and temperature [17]. A number of authors [43–45] have concluded that in basic media hydrolisis and condensation reactions occur simultaneously but that condensation is accelerated more than hydrolysis [44].

As TEOS hydrolysis and condensation in basic media are generally studied by raising the pH with the addition of NaOH, KOH or NH_4OH, the condensation product is SiO_2. The water hydrolysis and concomitant rise in pH taking place in cement phase dissolution (hastening TEOS or, where UCA-T is involved, silica oligomer hydrolysis), however, also releases calcium, silicon and aluminum ions into the solution. Consequently, the $Si(OH)_4$ resulting from UCA-T hydrolysis could react with those ions to generate calcium aluminosilicates. Several authors [3,7,12,13,46] have shown that $Si(OH)_4$, resulting from TEOS hydrolysis, can react with calcium ions or with portlandite yielding C–S–H gel, which is the prevalent phase in cement paste.

The heat released by sample PS-6% after 4 h 21 min (beginning of the induction period) was practically the same as the heat observed in PS after 4 h 48 min, the time of peak heat flow in its acceleration period (Table S2). The FTIR findings showed that at 4 h 21 min PS-6% had no portlandite but slightly higher absorption at 990 cm^{-1} to 970 cm^{-1}, a band characteristic of C–S–H gel. That would attest to alite hydration (exothermal reaction) and the reaction between the portlandite formed with the $Si(OH)_4$, giving rise to further C–S–H. At the same time portlandite consumption would stimulate alite dissolution and consequently C–S–H gel precipitation. That interpretation is further supported by the TG findings for the samples (Tables S1 and 5), for 4 h 21 min sample PS-6%, while lacking portlandite, contained 1.5-fold more bound water than the 4 h 48 min PS sample. Water loss was also observed in that sample at 750 °C–1000 °C, whilst no signal was detected in that temperature range on the PS thermogram recorded at 4 h 48 min.

Moreover, the TG/DTG curves for the three pastes contained signals for gypsum in the early hours of hydration, a finding confirmed by FTIR. They were more intense at 54 min in PS than in sample PS-6% at 29 min or 47 min (Fig. 12), possibly denoting a reaction with aluminates that would yield ettringite. Such interpretation would be supported by the mass loss recorded (Tables S1 and 5) and the DTG peak with a maximum at 70 °C–80 °C (Fig. 11), attributable not only to C–S–H but also to ettringite dehydration. The presence of UCA-T would appear to accelerate amorphous ettringite formation in early age hydration. The intense dissolution of C_3A in that stage would contribute to the new exothermal peak observed on the calorimetric curves for the UCA-T-containing pastes.

The new pre-induction exothermal peak present on the calorimetric curves for the UCA-T-bearing pastes, then, denotes C_3A and C_3S dissolution, both exothermal, UCA-T oligomer hydrolysis, exothermal in basic media, and C–S–H precipitation resulting from alite hydration and the reaction between hydrolysed silane and portlandite.

The findings suggest that while at time zero UCA-T lowers C_3A and C_3S dissolution, in just a few minutes such dissolution accelerates even though the beginning of the induction period is delayed. With the addition of UCA-T, the induction period is lengthened and the higher the silane content, the steeper the decline in the heat released at peak acceleration and in the total heat released after 24 h or 7 d of hydration.

5. Conclusions

- The addition of oligomeric ethoxisilane UCA-T modifies the hydration of cement at early age.

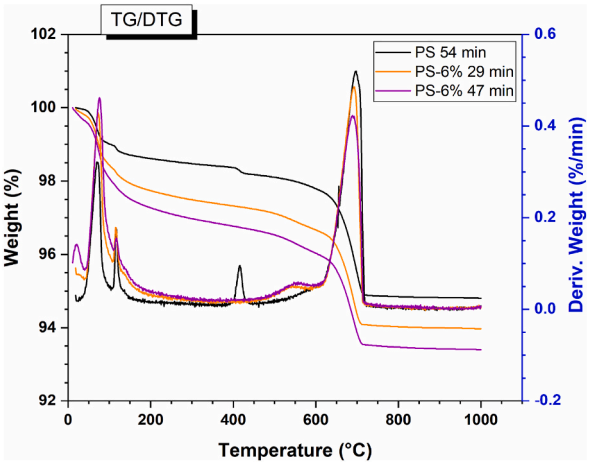

Fig. 12. TG/DTG curves for PS (54 min), PS-6% (47 min) and PS-6% (29 min).

- The calorimetric curve exhibits a new exothermal peak, in the pre-induction period, indicative of UCA-T hydrolysis, C_3A and C_3S dissolution and ettringite and C–S–H gel precipitation. Portlandite does not precipitate but reacts with the $Si(OH)_4$ sourced from UCA-T hydrolysis to generate further C–S–H gel.
- The induction period following on that new exothermal peak is considerably longer than the period observed in the reference cement, an effect that intensifies at higher UCA-T content. Further research is required to determine the causes for that development.
- The 7 d heat of hydration observed, 36% lower in the samples with 3% UCA-T than in the reference and 29% in the cement bearing 6% of the product, along with the decline in portlandite content, denotes a lower degree of hydration at that age in the samples bearing the product.
- Portlandite, does not precipitate but reacts with the $Si(OH)_4$ sourced from UCA-T hydrolysis to generate further C–S–H gel.

Author statement

N. Husillos-Rodríguez: Methodology, Writing- Original draft preparation., Discussion of the results; S. Martínez-Ramírez: Writing-Original draft preparation., Discussion of the results; RAFAEL ZARZUELA Methodology, Discussion of the results; M.J MOSQUERA: Discussion of the results; MARIA TERESA BLANCO VARELA. Conceptualization, Methodology, Writing- Original draft preparation., Discussion of the results; INES GARCIA LODEIRO: Conceptualization, Writing- Original draft preparation, Discussion of the results.

Declaration of competing interest

The authors declare the following financial interests/personal relationships which may be considered as potential competing interests:

All authors have participated in (a) conception and design, or analysis and interpretation of the data; (b) drafting the article or revising it critically for important intellectual content; and (c) approval of the final version.

This manuscript has not been submitted to, nor is under review at, another journal or other publishing venue.

The authors have no affiliation with any organization with a direct or indirect financial interest in the subject matter discussed in the manuscript.

The following authors have affiliations with organizations with direct or indirect financial interest in the subject matter discussed in the manuscript:

Acknowledgements

This study was funded by the European Union's Horizon H2020 Research and Innovation Programme under Grant Agreement No. 760858. Funding was also received from the Regional Government of Madrid, (S2018/NMT-4372 TOP Heritage-CM Programme). The support received from the CSIC's PTI-PAIS network during the roll-out of both projects is likewise gratefully acknowledged.

Appendix A. Supplementary data

Supplementary data to this article can be found online at https://doi.org/10.1016/j.jobe.2022.104127.

References

[1] B. Pigino, A. Leemann, E. Franzoni, P. Lura, Ethyl silicate for surface treatment of concrete part II: characteristics and performance, Cement Concr. Compos. 34 (2012) 313–321, https://doi.org/10.1016/j.cemconcomp.2011.11.021.

[2] E. Franzoni, B. Pigino, C. Pistolesi, Ethyl silicate for surface protection of concrete: performance in comparison with other inorganic surface treatments, Cement Concr. Compos. 44 (2013) 69–76, https://doi.org/10.1016/j.cemconcomp.2013.05.008.

[3] F. Sandrolini, E. Franzoni, B. Pigino, Ethyl silicate for surface treatment of concrete - part I: pozzolanic effect of ethyl silicate, Cement Concr. Compos. 34 (2012) 306–312, https://doi.org/10.1016/j.cemconcomp.2011.12.003.

[4] X. Pan, Z. Shi, C. Shi, T.-C. Ling, N. Li, A review on concrete surface treatment part I: types and mechanisms, Construct. Build. Mater. 132 (2017) 578–590, https://doi.org/10.1016/j.conbuildmat.2016.12.025.

[5] J.G. Dai, Y. Akira, F.H. Wittmann, H. Yokota, P. Zhang, Water repellent surface impregnation for extension of service life of reinforced concrete structures in marine environments: the role of cracks, Cement Concr. Compos. 32 (2010) 101–109, https://doi.org/10.1016/j.cemconcom.2009.11.001.

[6] P. Maravelaki-Kalaitzaki, N. Kallithrakas, D. Korakaki, Z. Agioutantis, S. Maurigiannakis, Evaluation of silicon-based strengthening agents on porous limestones, Prog. Org. Coating 57 (2006) 140–148, https://doi.org/10.1016/j.porgcoat.2006.08.007.

[7] A.M. Barberena-Fernández, P.M. Carmona-Quiroga, M.T. Blanco-Varela, Interaction of TEOS with cementitious materials: chemical and physical effects, Cement Concr. Compos. 55 (2015) 145–152, https://doi.org/10.1016/j.cemconcomp.2014.09.010.

[8] A.M. Barberena-Fernández, M.T. Blanco-Varela, P.M. Carmona-Quiroga, Use of nanosilica- or nanolime-additioned TEOS to consolidate cementitious materials in heritage structures: physical and mechanical properties of mortars, Cement Concr. Compos. 95 (2018) 271–276, https://doi.org/10.1016/j.cemconcomp.2018.09.011.

[9] P. Janez, R. Zarzuela, I. Garcia-Lodeiro, M.T. Blanco-Varela, M.J. Mosquera, T. Seemann, L. Yu, Modelling penetration depth of impregnation products for cementitious materials as a function of their pore size distribution, Construct. Build. Mater. 257 (2020) 119595, https://doi.org/10.1016/j.conbuildmat.2020.119595.

[10] P. Hou, R. Zhang, Y. Cai, X. Cheng, S.P. Shah, In situ $Ca(OH)_2$ consumption of TEOS on the surface of hardened cement-based materials and its improving effects on the Ca-leaching and sulfate-attack resistivity, Construct. Build. Mater. 113 (2016) 890–896, https://doi.org/10.1016/j.conbuildmat.2016.03.155.

[11] P. Hou, X. Cheng, J. Qian, S.P. Shah, Effects and mechanisms of surface treatment of hardened cement-based materials with colloidal nanoSiO_2 and its precursor, Construct. Build. Mater. 53 (2014) 66–73, https://doi.org/10.1016/j.conbuildmat.2013.11.062.

[12] R. Zarzuela, M. Luna, L.M. Carrascosa, M.P. Yeste, I. Garcia-Lodeiro, M.T. Blanco-Varela, M.A. Cauquic, J.M. Rodríguez-Izquierdo, M.J. Mosquera, Producing C-S-H gel by reaction between silica oligomers and portlandite: a promising approach to repair cementitious materials, Cement Concr. Res. 130 (2020) 106008, https://doi.org/10.1016/j.cemconres.2020.106008.

[13] I. Garcia-Lodeiro, P.M. Carmona-Quiroga, R. Zarzuela, M.J. Mosquera, M.T. Blanco-Varela, Chemistry of the interaction between an alkoxysilane-based impregnation treatment and cementitious phases, Cement Concr. Res. 142 (2021) 106351, https://doi.org/10.1016/j.cemconres.2020.106351.

[14] M.J. McCarthy, T.D. Dyer, Pozzolanas and pozzolanic materials, in: P.C. Hewlett, M. Liska, Lea's (Eds.), Chemistry of Cement and Concrete, fifth ed., Butterworth-Heinemann, 2019, ISBN 9780081007730, pp. 363–467, https://doi.org/10.1016/B978-0-08-100773-0.00009-5.

[15] M. Schmidt, E. Fehling, Ultra-high-performance concrete: research, development and application in Europe, ACI Spec. Publ. 228 (2005) 51–78.

[16] J. Zelić, D. Rušiš, D. Veza, R. Krstulovi, The role of silica fume in the kinetics and mechanisms during the early stage of cement hydration, Cement Concr. Res. 30 (2000) 1655–1662, https://doi.org/10.1016/S0008-8846(00)00374-4.

[17] R. Aelion, A. Loebel, F. Eirich, Hydrolysis of ethyl silicate, J. Am. Chem. Soc. 72 (1950) 5705–5712, https://doi.org/10.1021/ja01168a090.

[18] X.M. Kong, H. Liu, Z.B. Lu, D.M. Wang, The influence of silanes on hydration and strength development of cementitious systems, Cement Concr. Res. 67 (2015) 168–178, https://doi.org/10.1016/j.cemconres.2014.10.008.

[19] Y. Cai, P. Hou, C. Duan, R. Zhang, Z. Zhou, X. Cheng, S. Shah, The use of tetraethyl orthosilicate silane (TEOS) for surface-treatment of hardened cement-based materials: a comparison study with normal treatment agents, Construct. Build. Mater. 117 (2016) 144–151, https://doi.org/10.1016/j.conbuildmat.2016.05.028.

[20] H. Feng, H.T.N. Le, S. Wanga, M.H. Zhang, Effects of silanes and silane derivatives on cement hydration and mechanical properties of mortars, Construct. Build. Mater. 129 (2016) 48–60, https://doi.org/10.1016/j.conbuildmat.2016.11.004.

[21] B. Koohestani, Effect of saline admixtures on mechanical and microstructural properties of cementitious matrices containing tailings, Construct. Build. Mater. 156 (2017) 1019–1027, https://doi.org/10.1016/j.conbuildmat.2017.09.048.

[22] B. Chen, H. Shao, B. Li, Z. Li, Influence of silane on hydration characteristics and mechanical properties of cement paste, Cement Concr. Compos. 113 (2020) 103743, https://doi.org/10.1016/j.cemconcomp.2020.103743.

[23] D.S. Facio, M. Luna, M.J. Mosquera, Facile preparation of mesoporous silica monoliths by an inverse micelle mechanism, Microporous Mesoporous Mater. 247 (2017) 166–176, https://doi.org/10.1016/j.micromeso.2017.03.041.

[24] M.J. Mosquera, J.F. Illescas, D.S. Facio, International Patent. No. WO2013/121058, 2014. February 14.

[25] F. Winnefeld, A. Schöler, B. Lothenbach, Sample preparation (chapter 1), in: K. Scrivener, R. Snellings, B. Lothenbach (Eds.), A Practical Guide to Microstructural Analysis of Cementitious Materials, CRC Press, 2016, https://doi.org/10.1201/b19074. Taylor & Francis Group.

[26] C.A. Casagrande, L.F. Jochem, L. Onghero, P.R. de Matos, W.L. Repette, P.J.P. Gleize, Effect of partial substitution of superplasticizer by silanes in Portland cement pastes, J. Build. Eng. 29 (2020) 101226, https://doi.org/10.1016/j.jobe.2020.101226.

[27] I. Garcia-Lodeiro, S. Gonzalez-Aguza, R. Zarzuela, Y. Pardos, R. Garcia-Navarro, A. Tébar, M.J. Mosquera, M.T. Blanco-Varela, Studying the dosage-dependent influence of hydrophobic alkoxysilane/siloxane admixtures on the performance of repair micromortars, J. Build. Eng. 48 (2022) 103905, https://doi.org/10.1016/j.jobe.2021.103905.

[28] G. Collodetti, P.J.P. Gleize, P.J.M. Monteiro, Exploring the potential of siloxane surface modified nano-SiO_2 to improve the Portland cement pastes hydration properties, Construct. Build. Mater. 54 (2014) 99–105, https://doi.org/10.1016/j.conbuildmat.2013.12.028.

[29] F. Švegl, J. Šuput-Strupi, L. Škrlep, K. Kalcher, The influence of aminosilanes on macroscopic properties of cement paste, Cement Concr. Res. 38 (2008) 945–954, https://doi.org/10.1016/j.cemconres.2008.02.006.

[30] F. Puertas, H. Santos, M. Palacios, S. Martínez-Ramirez, Polycarboxylatesuperplasticizer admixtures: effect on hydration, microstructure and rheological behaviour in cement pastes, Adv. Cement Res. 17 (2) (2005) 77–89, https://doi.org/10.1680/adcr.2005.17.2.77.

[31] M.M. Alonso, M. Palacios, F. Puertas, Compatibility between polycarboxylate-based admixtures and blended-cement pastes, Cement Concr. Compos. 35 (2013) 151–162, https://doi.org/10.1016/j.cemconcomp.2012.08.020.

[32] B. Lothenbach, P. Durdziński, K. De Weerdt, in: K. Scrivener, R. Snellings, B. Lothenbach (Eds.), Thermogravimetric Analysis in A Practical Guide to Microstructural Analysis of Cementitious Materials, CRC Press, Taylor & Francis Book, Scrivener, 2016.

[33] T. Grounds, H.G. Midgley, D.V. Nowell, The use of thermal methods to estimate the state of hydration of calcium trisulphoaluminate hydrate $3CaO{\cdot}Al_2O_3{\cdot}3\text{-}CaSO_4{\cdot}nH_2O$, Thermochim. Acta 85 (1985) 215–218, https://doi.org/10.1016/0040-6031(85)85567-2.

[34] R. Gabrovšek, T. Vuk, V. Kaučič, The preparation and thermal behavior of calcium monocarboaluminate, Acta Chim. Slov. 55 (2008) 942–950.

[35] P. Yu, R.J. Kirkpatrick, B. Poe, P.F. McMillan, X. Cong, Structure of calcium silicate hydrate (C-S-H): near-, mid-, and far-infrared spectroscopy, J. Am. Ceram. Soc. 82 (3) (1999) 742–748, https://doi.org/10.1111/j.1151-2916.1999.tb01826.x.

[36] S. Martinez-Ramirez, M. Frías, C. Domingo, Micro-Raman spectroscopy in white portland cement hydration: long-term study at room temperature, J. Raman Spectrosc. 37 (2006) 555–561, https://doi.org/10.1002/jrs.1428.

[37] D. Torréns-Martín, L. Fernández-Carrasco, S. Martínez-Ramírez, J. Ibáñez, L. Artús, T. Matschei, Raman spectroscopy of anhydrous and hydrated calcium aluminates and sulfoaluminates, J. Am. Ceram. Soc. 96 (11) (2013) 3589–3595, https://doi.org/10.1111/jace.12535.

[38] G. Socrates, Infrared and Raman Characteristic Group Frequencies, third ed., John Wiley and Sons, LTD, England, 2006.

[39] S.C.B. Myneni, S.J. Traina, G.A. Waychunas, T.J. Logan, Vibrational spectroscopy of functional group chemistry and arsenate coordination in ettringite, Geochem. Cosmochim. Acta 62 (1998) 3499–3514, https://doi.org/10.1016/S0016-7037(98)00221-X.

[40] R. Al-Oweini, H. El-Rassy, Synthesis and characterization by FTIR spectroscopy of silica aerogels prepared using several $Si(OR)_4$ and $R''Si(OR')_3$ precursors, J. Mol. Struct. 919 (2009) 140–145, https://doi.org/10.1016/j.molstruc.2008.08.025.

[41] J.W. Bullard, H.M. Jennings, R.A. Livingston, A. Nonat, G.W. Scherer, J.S. Schweitzer, K.L. Scrivener, J.J. Thomas, Mechanisms of cement hydration, Cement Concr. Res. 41 (2011) 1208–1223, https://doi.org/10.1016/j.cemconres.2010.09.011.

[42] J. Matsuoka, M. Numaguchi, S. Yoshida, N. Soga, Heat of reaction of the hydrolysis-polymerization process of tetraethyl orthosilicate in acidic condition, J. Sol. Gel Sci. Technol. 19 (1) (2000) 661–664, https://doi.org/10.1023/A:1008746318901.

[43] B.E. Yoldas, Transparent porous alumina, Am. Ceram. Soc. Bull. 54 (1975) 286–288.

[44] Y. Xu, X. Sun, D. Wu, Y. Sun, Y. Yang, H. Yuan, F. Deng, Z. Wu, Ammonia catalyzed hydrolysis-condensation kinetics of tetraethoxysilane// dimethyldiethoxysilane mixtures studied by 29Si NMR and SAXS, J. Solut. Chem. 36 (2007) 327–344, https://doi.org/10.1007/S10953-006-9117-Y.

[45] C.J. Brinker, Hydrolysis and condensation of silicates: effects on structure, J. Non-Cryst. Solids 100 (1988) 31–50, https://doi.org/10.1016/0022-3093(88)90005-1.

[46] A. Moropoulou, A. Cakmak, K.C. Labropoulos, R. Van Grieken, K. Torfs, Accelerated microstructural evolution of a calcium–silicate–hydrate (C–S–H) phase in pozzolanic pastes using fine siliceous sources: comparison with historic pozzolanic mortars, Cement Concr. Res. 34 (2004) 1–6, https://doi.org/10.1016/S0008-8846(03)00187-X.